Pramāna – J. Phys., Vol. 29, No. 6, December 1987, pp. 559–575. © Printed in India.

Four quasi-particle level at 2256 keV in ^{182}Re

Y K AGARWAL, C V K BABA, D BHATTACHARYA, S K BHATTACHERJEE, R K BHOWMIK*, V M DATAR†, H C JAIN and A ROY

Tata Institute of Fundamental Research, Homi Bhabha Road, Bombay 400005, India
*Present address: Nuclear Science Centre, New Delhi 110067, India
†Nuclear Physics Division, Bhabha Atomic Research Centre, Trombay, Bombay 400085, India

MS received 7 August 1987

Abstract. In-beam nuclear spectroscopic studies of ^{182}Re, following the reaction ^{181}Ta(α, $3n$)^{182}Re have been made using gamma-ray and internal conversion electron techniques. K-conversion coefficients for several transitions have been measured and the multipolarities of the various transitions assigned. In particular, the spin and parity of the four-quasi-particle isomeric level at 2256 keV were determined to be 16^-. The g-factor of this level has been measured to be $g = 0{\cdot}32 \pm 0{\cdot}05$. On the basis of the g-factor and the decay pattern of this level, a configuration $\{\nu 9/2^+[624\uparrow]\nu 7/2^-[514\downarrow]\nu 7/2^-[503\uparrow]\pi 9/2^-[514\uparrow]\}_{K^\pi=16^-}$ has been assigned to this level. The nature of the retardation of the gamma transitions deexciting this level is discussed. It is argued that the measured retardation factors can be explained if the nucleus has a triaxial shape.

Keywords. Nuclear reactions: ^{181}Ta(α, $3n$)^{182}Re; gamma-ray; internal conversion electron spectroscopy; internal conversion coefficients; g-factor; triaxial deformation.

PACS Nos 21·10; 25; 21·60

1. Introduction

Extensive investigations have been made on even-even and odd mass deformed nuclei up to high spins; however, relatively little work has been reported on odd-odd deformed nuclei. The high level density and the consequent complexity of the spectra are some of the reasons for the paucity of data on these nuclei. Recently, Slaughter *et al* (1984) investigated the odd-odd deformed nucleus ^{182}Re through gamma-ray spectroscopy following the ^{181}Ta(α, $3n$)^{182}Re reaction. Earlier, this nucleus was studied through the radioactive decay of ^{182}Os (Burson *et al* 1973; Svahn *et al* 1973; Lederer and Shirley 1978) and through in-beam gamma-ray studies (Hjorth *et al* 1968; Medsker *et al* 1971). Slaughter *et al* (1984) identified four rotational bands, built on two quasi-particle states; with K^π-values of 7^+, 9^-, 2^+ and 4^-. The level sequence proposed by them is shown in figure 1. They also assigned the band heads on the basis of Nilsson states available near the Fermi level. In addition, they identified an isomeric level at 2256 keV with a half-life of (88 ± 8)nsec (in the text and the figures, the energies of the transitions and the levels have been rounded off to the nearest keV. The exact energies of the transitions with the estimated uncertainties are quoted in table 1). This level was identified as a 3-proton-1-neutron four-quasi-particle state. Probable assignments on the basis of Nilsson orbitals were made and it was concluded that the state is most probably the band head of a $K^\pi = 15^+$ band with the configuration

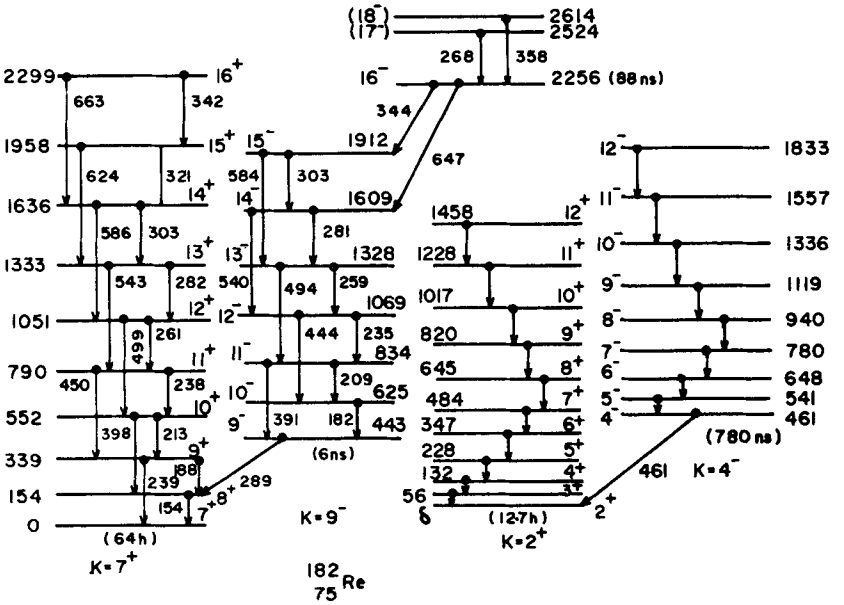

Figure 1. Level scheme of ^{182}Re populated in the ^{181}Ta(α, $3n$)^{182}Re reaction as proposed by Slaughter *et al* (1984). The energies of the levels are given in keV. The exact energies of the transitions in the $K^{\pi} = 9^-$ and 7^+ bands are given in table 1. The spins and parities of the 2256, 2524 and 2614 keV levels are deduced from the present work. The location of the 2^+ band-head is not known and is denoted by δ. The energies of all the levels in the 2^+ and 4^- bands thus have to be increased by δ with respect to the energies shown in the figure.

$\pi 9/2^-[514\uparrow]\pi 7/2^-[523\uparrow]\pi 5/2^+[402\uparrow]\nu 9/2^+[624\uparrow]$. The transition probabilities of the electromagnetic transitions from this level to the excited levels of the $K^{\pi} = 9^-$ band were invoked in arriving at this assignment. While angular distribution was studied by Slaughter *et al* (1984) to infer the multipolarities and mixing ratios of the transitions, no data exist on the internal conversion coefficients for these transitions.

In the present work, the levels in ^{182}Re have been studied through in-beam gamma-ray and internal conversion electron spectroscopy following the ^{181}Ta(α, $3n$)^{182}Re reaction. Attention was directed only at the 7^+ and 9^- bands and on the isomeric level. Internal conversion coefficients of the transitions between these levels were measured. Further, the magnetic moment of the isomeric level at 2256 keV was measured in order to elucidate its nature. A preliminary report of the g-factor measurement was presented earlier (Agarwal *et al* 1985).

2. Experimental details

2.1 *Target and the beam*

A natural Ta foil of high purity (> 99·9%) was rolled to a thickness of 1·7 mg/cm^2. This self-supporting target, of dimensions 2 × 2 cm, was used in the gamma-ray and conversion-electron spectroscopic studies. A 0·075 mm thick Ta foil backed by a ^{208}Pb foil thick enough to stop an α-beam of 45 MeV was used in the g-factor studies.

α-beam with energies of 40 MeV and 42 MeV were used for the spectroscopic and *g*-factor studies respectively. The beam current used was between 0·5 and 4·0 nA in all the experiments. The experiments were performed at the Variable Energy Cyclotron Centre (VECC) at Calcutta.

2.2 *Single gamma-ray spectra*

The single gamma-ray spectra were measured using a 25% HPGe detector. In this experiment, the target was placed at the centre of a long cylindrical chamber with 10 cm dia, the beam entering and exiting at an angle of 45° to the axis of the cylinder. The detector, with its front surface at 8 cm from the target, was kept at an angle 45° to the beam direction. A 1 mm thick Cd absorber was placed in front of the detector. The beam was focussed to a size of 2 mm dia on the target. The energy and efficiency calibrations of the detector were obtained by recording and analyzing the known gamma-ray spectrum of a ^{152}Eu source kept at the target position. A typical gamma-ray spectrum obtained in the present experiment is shown in figure 2. Apart from the gamma transitions in ^{182}Re, several lines due to transitions in ^{181}Re populated through the $(\alpha, 4n)$ reaction are also seen in this spectrum. These lines were identified from the work of Singh *et al* (1974). Coincidence experiments provided further confirmation for transitions assigned to ^{182}Re.

2.3 *Internal conversion electron and electron-gamma coincidence measurements*

The internal conversion electron spectra were measured with a solenoidal transport spectrometer fabricated in our laboratory. A schematic diagram of the spectrometer is shown in figure 3. It consists of a 100 cm long solenoid around a stainless steel tube of internal diameter of 5 cm. The target and the Si(Li) detector [dia 20 mm and thickness 3 mm] are in the magnetic field region. A central circular stopper (a disc of dia 6 mm) prevents the low energy δ-electrons from reaching the Si(Li) detector. The electrons from the target follow helical trajectories in the axial magnetic field and reach the Si(Li) detector, where their energy spectrum is measured. The maximum magnetic field obtainable was 0·4 T corresponding to a current of 500 A in the coils, which were cooled by chilled water circulating in the water jacket surrounding them (see figure 3). The overall energy resolution, determined mainly by the target thickness in the present case, is 4 keV. A single-ended co-axial Ge(Li) detector, which can operate in a magnetic field without a deterioration of its performance, was kept at a distance of ≈ 3 cm from the target. This arrangement allows one to measure electron-gamma coincidence spectra with good efficiency. The energy calibration for the Si(Li) detector as well as the Ge(Li) detector and the transmission of the spectrometer were measured by recording spectra from ^{152}Eu, ^{207}Bi and ^{137}Cs sources of known strengths, kept at the target position in the spectrometer. The measured transmission of the solenoid spectrometer as a function of the electron energy is shown in figure 4. It should be noted that the curve in figure 4 corresponds to the specific magnetic field range and the Si(Li) detector used. For a detector of a different size and/or for a different range of the magnetic field, the efficiency curve would be different.

The α-beam, focussed to a size of 2 mm dia on the target, was incident normal to the target surface. The beam transmitted through the target was dumped in a well-shielded Faraday-cup kept at a distance of 2 m downstream. Care had to be taken in positioning the beam dump and the beam-line tube leading to it, because of the

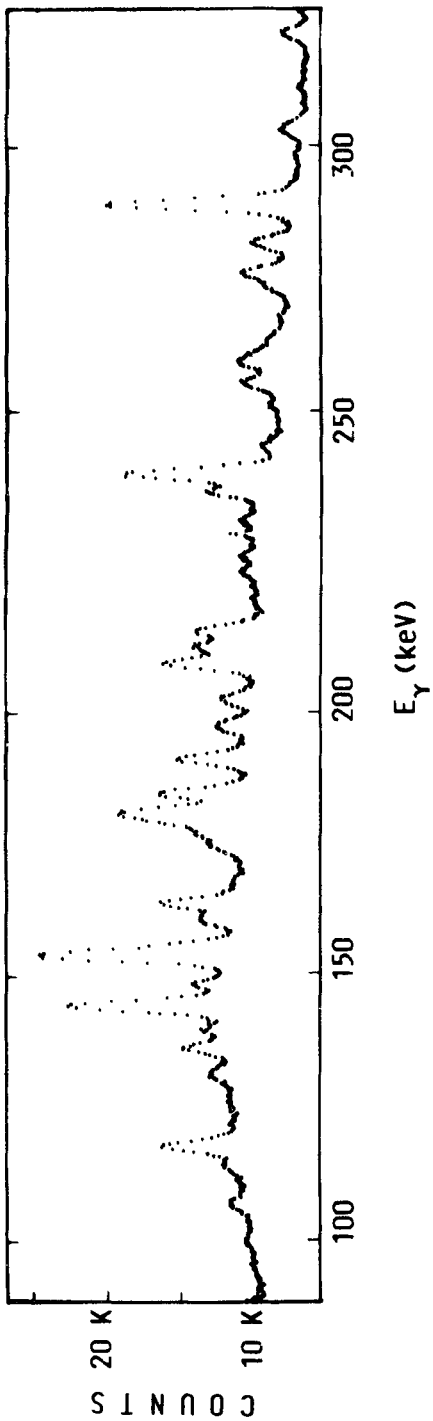

Figure 2.

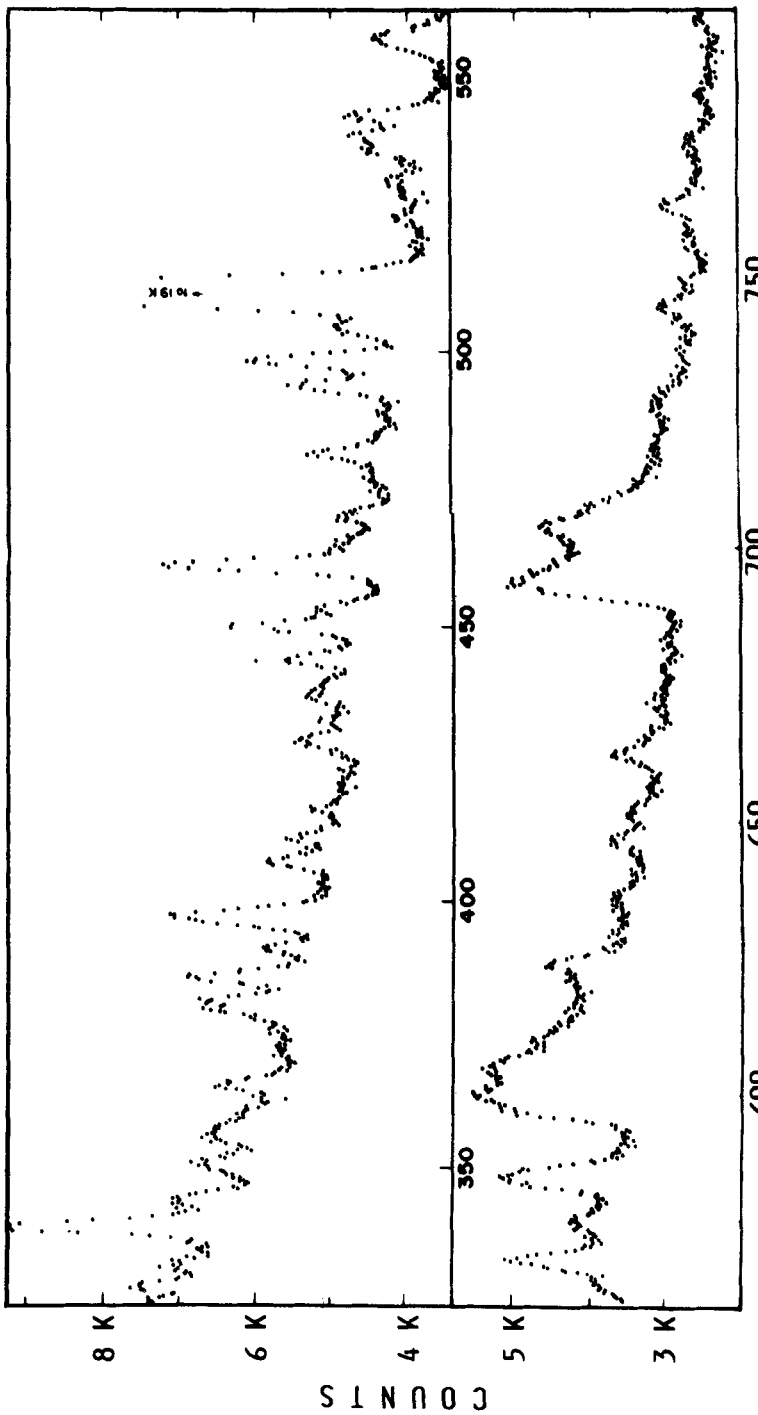

Figure 2. Singles gamma-ray spectrum taken with a 25% HPGe detector with 1 mm thick Cd absorber in front of the detector.

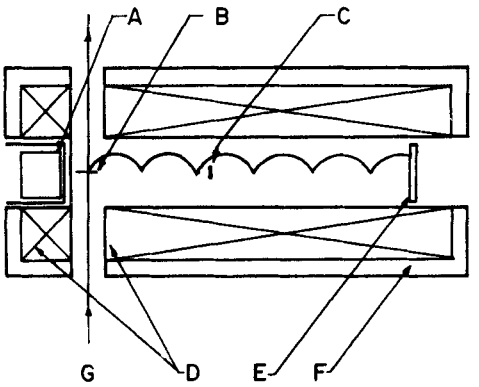

Figure 3. Schematic diagram of the Solenoid electron spectrometer used in the present investigation (not to scale). The various components are marked in the figure **A**: Ge(Li) detector, **B**: target, **C**: central stopper, **D**: coil of the solenoid, **E**: Si(Li) detector, **F**: cooling water jacket, **G**: the beam. A typical electron trajectory is shown in the figure.

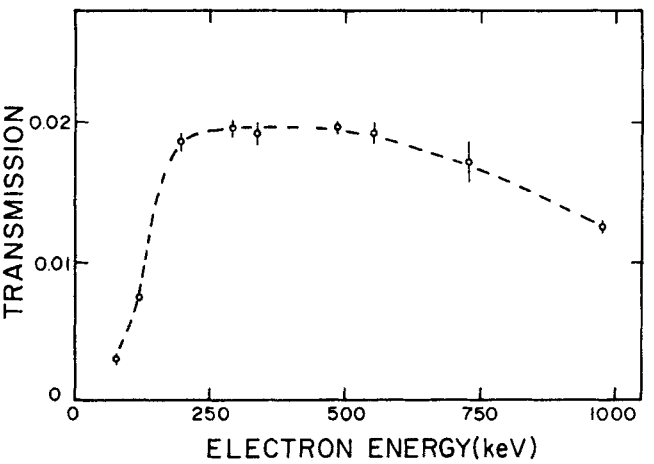

Figure 4. Transmission (number of counts detected in the electron peak divided by the number of electrons emmitted by the source) of the solenoid electron spectrometer as a function of the electron energy, for the Si(Li) detector used and the range of the magnetic field used in the present experiment.

bending of the α-beam in the magnetic field of the solenoid. The vacuum in the entire spectrometer was better than 4×10^{-6} torr. A typical singles internal conversion electron spectrum following the $\alpha + Ta$ reaction obtained with the above spectrometer, is shown in figure 5. The current in the coil was varied between 200 and 300 A, in short-time intervals for this measurement.

Coincidence spectra of the internal conversion electrons detected in the Si(Li) detector of the solenoid spectrometer and gamma-rays detected in the Ge(Li) detector were recorded using a Canberra series 88 multi-parameter data acquisition system. The parameters recorded were: (i) energy of electrons, (ii) energy of the gamma-rays,

(iii) the time, e^- vs RF and (iv) the time, e^- vs γ. The data were written in an event-by-event mode on a magnetic tape. The resolving time was 25 nsec for the e-γ time spectrum and 12 nsec for the e-RF time spectrum.

2.4 *Gamma-gamma coincidence measurement with a multiplicity filter*

A gamma-gamma coincidence measurement with a multiplicity filter was made, in an attempt to identify transitions feeding the isomeric level, using two HPGe detectors [25% and 30% efficiencies] and a set of six 5 cm thick × 4 cm dia NaI(Tl) detectors. The NaI(Tl) detectors, kept at 8 cm distance from the target, served as a multiplicity filter. The timing signals of the NaI(Tl) detectors were matched to better than 1 nsec and were fed into a multiplicity selection unit fabricated in our laboratory. The unit was set to give an output if two or more of the NaI(Tl) detectors fired within 20 nsec of each other. This output together with a pulse derived from the cyclotron RF were fed into a time-to-amplitude converter (TAC) unit to give time information of the events detected in NaI(Tl) detectors with respect to the RF. Five-parameter data, consisting of the gamma-ray energies in the two HPGe detectors, the output of the above mentioned multiplicity filter-RF TAC and the time information of the two HPGe detectors with respect to the cyclotron RF, were collected on a magnetic tape event by event. The data were sorted and analysed off-line. Due to limitations of the beam time and data collection speed only a limited amount of data could be obtained with this set-up. The result obtained from such an analysis is discussed in § 3.1.

2.5 *g-factor measurement*

The g-factor of the 2256 keV level was measured by a time differential perturbed angular distribution method (see e.g. Frauenfelder and Steffen 1965) in an external magnetic field. A Ta target backed by a ^{208}Pb stopper, described in § 2.1 was placed in a small vacuum chamber placed between the pole faces of an electromagnet. The uniformity of the magnetic field was measured to be within 1% over the pole gap and over the central area of the pole-faces. The two HPGe detectors were kept at a distance of 15 cm from the target, at $\pm 135°$ with respect to the beam direction. Two-dimensional spectra of energy vs time were measured for each of the detectors. The relative efficiencies of the two detectors were determined by measuring the singles gamma-ray spectra without the magnetic field. The efficiency corrected counting rates $N_+(t)$ and $N_-(t)$ for the two detectors at $\pm 135°$ were extracted from the two parameter spectra for 345 and 647 keV transitions which deexcite the isomeric level. These counting rates were used to form the ratio

$$R(t) = \frac{N_+(t) - N_-(t)}{N_+(t) + N_-(t)}. \tag{1}$$

The ratio plotted as a function of t, the time of the gamma-ray emission after the formation of the level, contains information on the g-factor through the relation

$$R(t) = \frac{0{\cdot}75\, A_2}{1 + 0{\cdot}25\, A_2} \sin 2\omega t, \tag{2}$$

where A_2 is the coefficient of $P_2(\cos\theta)$ in the Legendre polynomial expansion of the

angular distribution of the gamma-ray and ω is the Larmor precision frequency given by

$$\omega = -\mu B/I\hbar. \tag{3}$$

In the above expression B is the magnetic field acting at the site of the nucleus and μ, the magnetic moment of the isomer ($\mu = gI$, I being the nuclear spin).

The whole system was tested by measuring the well-known magnetic moment of the 2188 keV (8^+) level in ^{210}Po, (Lederer and Shirley 1978) which was formed simultaneously through the ^{208}Pb (α, $2n$)^{210}Po reaction on the ^{208}Pb backing of the Ta target. From the known g-factor of this level, a value of $1{\cdot}62 \pm 0{\cdot}04$ T was obtained for the magnetic field. This was in agreement with the field measured with a calibrated Hall effect Gaussmeter.

3. Results

3.1 *Electron-gamma and gamma-gamma coincidence measurements*

The four-parameter data on conversion electron-gamma coincidence measurements were analysed off-line by selecting various gamma, electron and time gates. The resulting spectra confirmed the level sequences proposed by Slaughter *et al* (1984). These have been utilized to obtain reliable conversion coefficients for some of the transitions (see § 3.2).

An attempt was also made to identify transitions feeding the isomeric level by the technique described in § 2.4. A four-fold coincidence spectrum (prompt) in one of the HPGe detectors, with the requirement that at least two of the six NaI(Tl) detectors have delayed events and that the other HPGe detector has a delayed transition of the 9^- band (see figure 1), is shown in figure 6. Even with the limited statistics, the spectrum clearly shows that 268 and 358 keV transitions feed the isomeric level. Better statistics could not be obtained due to limitations mentioned in § 2.4.

3.2 *Internal conversion coefficients*

The singles internal conversion electron and gamma-spectra resulting from a 40 MeV α-beam incident on a $1{\cdot}7$ mg/cm^2 ^{181}Ta target are shown in figures 5 and 2 respectively. The strongest line at 296 keV seen in figure 5 is the K-conversion line of the 366 keV transition in ^{181}W populated in the radioactive decay of ^{181}Re produced by (α, $4n$) reaction on the Ta target. The intensities of transitions above 200 keV derived from the electron spectrum are listed in table 1. Also listed in table 1 are the intensities of some of the γ-transitions normalized to 100 for the 289 keV γ-transition. The electron intensities are normalized so that this transition has the theoretical K-conversion coefficient for an E1 multipolarity (Slaughter *et al* 1984). There is an overall agreement between the intensities obtained in the present work and that of Slaughter *et al* (1984) except for the intensities of the transitions deexciting the highest spin states. This difference is presumably because of the lower energy (38 MeV) of the α-beam used by Slaughter *et al* (1984). A higher energy was used in the present work intentionally so as to obtain a larger feed to the high spin levels. From the measured gamma-ray and electron intensities, the K-conversion coefficients (α_K) for several of the transitions were calculated and are listed in the last column of table 1. The

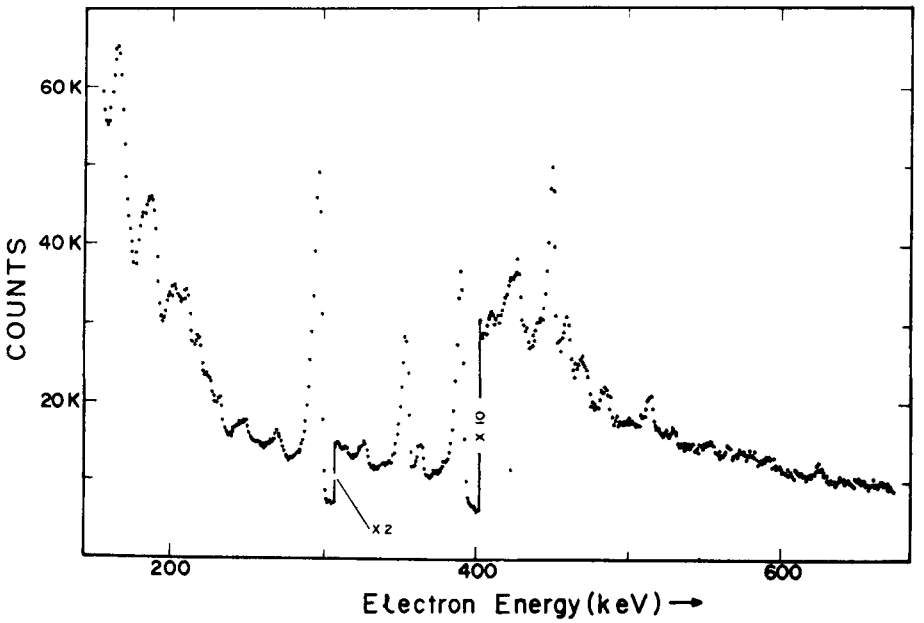

Figure 5. Singles internal conversion electron spectrum measured with the solenoid electron spectrometer, following the reaction $^{181}Ta + \alpha$.

experimental values of α_K are compared with the theoretical values of Hager and Seltzer (1968) for various multipolarities in figure 7. The correctness of the normalization procedure is verified by the agreement of the measured α_K's with the theoretical values for several of the transitions expected to be of E2 nature and for the 461 keV $M2$ transition (see figure 1). In order to emphasize the transitions deexciting the isomeric level, a delayed electron spectrum (delayed 15 to 100 nsec with respect to the RF) and coincident with the whole of the gamma-ray spectrum, was projected from the four-parameter data and is shown in figure 8. It can be seen that this spectrum essentially consists of transitions of the 9^- band as well as the 345 keV and 647 keV transitions deexciting the isomeric level. Utilizing the branching ratios as obtained from the measured gamma-ray intensities and assuming a multiplicity of two above the isomer, the multiplicities of the gamma-rays coincident with the 289, 345 and 647 keV transitions were calculated. The relative conversion coefficients of these transitions were obtained by dividing the observed electron intensities in the delayed spectrum by the multiplicities so calculated. The α_K's so obtained are listed in table 1 with remark 'a'. Further, the α_K's for the 268 and 358 keV transitions feeding the isomer were determined from a prompt electron spectrum in coincidence with all the gamma-rays. The internal conversion coefficients obtained in this manner confirm the assignments made by Slaughter *et al* (1984) for the transitions in the $K^\pi = 7^+$ and 9^- bands. The α_K's obtained for the 345 keV and 647 keV transitions are $0{\cdot}082 \pm 0{\cdot}008$ and $0{\cdot}0086 \pm 0{\cdot}0014$ respectively showing a $(M1 + E2)$ nature for the 345 keV transition and an $E2$ nature for 647 keV transition. These assignments fix the parity of the isomeric level as negative. Further, the measured α_K for the 345 keV transition implies an $E2$ admixture of $0{\cdot}58 \pm 0{\cdot}08$. The angular distribution coefficients for the 345 and 647 keV transitions were calculated with the above mixing ratio for the 345 keV

Table 1. Gamma-ray and K-conversion electron intensities and the K conversion coefficients α_K for various transitions in ^{182}Re observed through the reaction ^{181}Ta(α, $3n$)^{182}Re. The gamma-ray intensities are normalized to that of the 289 keV transition (100). The K-electron intensities are normalized such that K-conversion coefficient of the 289 keV transition is equal to the theoretical value of α_K for an E1 transition. The uncertainty in the transition energy is ± 0.3 keV unless otherwise indicated. The number in the paranthesis in the last column indicates the power to which 10 is raised to multiply the number given in the column.

Transition energy (keV) and placement in the level scheme	Gamma-ray intensity		K-conversion electron intensity	α_K
	Slaughter *et al* (1984)	Present Work		
154·3 ($8^+ \rightarrow 7^+$)	80 ± 5	80 ± 7		
185·1 ($9^+ \rightarrow 8^+$)	36 ± 2	38 ± 3		
339·3 ($9^+ \rightarrow 7^+$)	*	*		
212·5 ($10^+ \rightarrow 9^+$)	23 ± 2	26 ± 3		
397·5 ($10^+ \rightarrow 8^+$)	17 ± 1	18·0 ± 1·5	0·48 ± 0·06	2·7 ± 0·2 (−2)
237·7 ($11^+ \rightarrow 10^+$)	16 ± 1	*		
450·0 ($11^+ \rightarrow 9^+$)	18 ± 1	18 ± 1	0·41 ± 0·05	2·3 ± 0·5 (−2)
261·0 ($12^+ \rightarrow 11^+$)	8·9 ± 0·5	*		
498·5 ($12^+ \rightarrow 10^+$)	21 ± 1	20·0 ± 1·5	0·41 ± 0·05	2·1 ± 0·3 (−2)
282·3 ($13^+ \rightarrow 12^+$)	6 ± 1	5 ± 1	1·13 ± 0·15	2·3 ± 0·5 (−1)
543·4 ($13^+ \rightarrow 11^+$)	13 ± 1	12·0 ± 1·5	0·135 ± 0·015	1·13 ± 0·15 (−2)
303·6 ($14^+ \rightarrow 13^+$)	10·0 ± 1·5	12·0 ± 1·5	0·90 ± 0·12	7·4 ± 1·3 (−2)
303·0 ($15^- \rightarrow 14^-$)				
585·7 ($14^+ \rightarrow 12^+$)	13·0 ± 0·8	11 ± 1	0·14 ± 0·02	1·25 ± 0·21 (−2)
321·3 ($15^+ \rightarrow 14^+$)	(5·0 ± 0·3)*	12*	1·28 ± 0·12	1·07 ± 0·14 (−1)
624·4 ($15^+ \rightarrow 13^+$)	9 ± 1	10 ± 1	0·071 ± 0·012	7·1 ± 1·7 (−3)
341·7 ($16^+ \rightarrow 15^+$)	2·0 ± 0·2	4 ± 1		
662·8 ($16^+ \rightarrow 14^+$)	3·6 ± 0·3	8 ± 1	0·067 ± 0·011	8·4 ± 1·7 (−3)
181·5 ($10^- \rightarrow 9^-$)	43 ± 3	60 ± 5		
209·2 ($11^- \rightarrow 10^-$)	37 ± 2	40 ± 4		
390·9 ($11^- \rightarrow 9^-$)	5·1 ± 0·3	5·5 ± 0·5	0·19 ± 0·04	3·45 ± 0·85 (−2)
234·7 ($12^- \rightarrow 11^-$)	23 ± 1	19 ± 2		
443·8 ($12^- \rightarrow 10^-$)	9·2 ± 0·6	9·2 ± 0·8	0·23 ± 0·06	2·5 ± 0·7 (−2)
258·9 ($13^- \rightarrow 12^-$)	15 ± 1	(23 ± 3)*		
493·6 ($13^- \rightarrow 11^-$)	11 ± 1	14·0 ± 1·5	0·26 ± 0·04	1·86 ± 0·29 (−2)
281·1 ($14^- \rightarrow 13^-$)	11 ± 1	(20 ± 1·5)*		
540·0 ($14^- \rightarrow 12^-$)	8·4 ± 0·5	10 ± 0·8	0·16 ± 0·02	1·6 ± 0·3 (−2)
383·8 ($15^- \rightarrow 13^-$)	6·9 ± 0·5	12·0 ± 1·5	0·10 ± 0·02	8·3 ± 2·0 (−3)
288·9 ($9^- \rightarrow 8^+$)	100	100 (normalization)	2·25 (normalization)	2·25 (−2) (normalization)
344·3 ± 0·6 ($16^- \rightarrow 15^-$)	3·4 ± 0·3	7·5 ± 1·0	a	8·2 ± 0·8 (−2)
647·1 ($16^- \rightarrow 14^-$)	4·9 ± 0·4	6·1 ± 0·7	a	8·6 ± 1·4 (−3)
268·0 ± 0·5	3·2 ± 0·2	3·0 ± 0·4	b	2·2 ± 0·6 (−1)
358·5 ± 0·8	1·5 ± 0·2	2·5 ± 0·6	b	4·3 ± 1·4 (−2)
460·8 ($4^- \rightarrow 2^+$)	33 ± 2	6·0 ± 0·3	1·93 ± 0·12 (−1)	

* These lines have contribution from ^{181}Re produced through the (α, $4n$) reaction on ^{181}Ta.

[a] α_K obtained from delayed electron spectrum coincident with the total gamma-ray spectrum (see text).

[b] α_K obtained from the total conversion electron projection spectrum (see text).

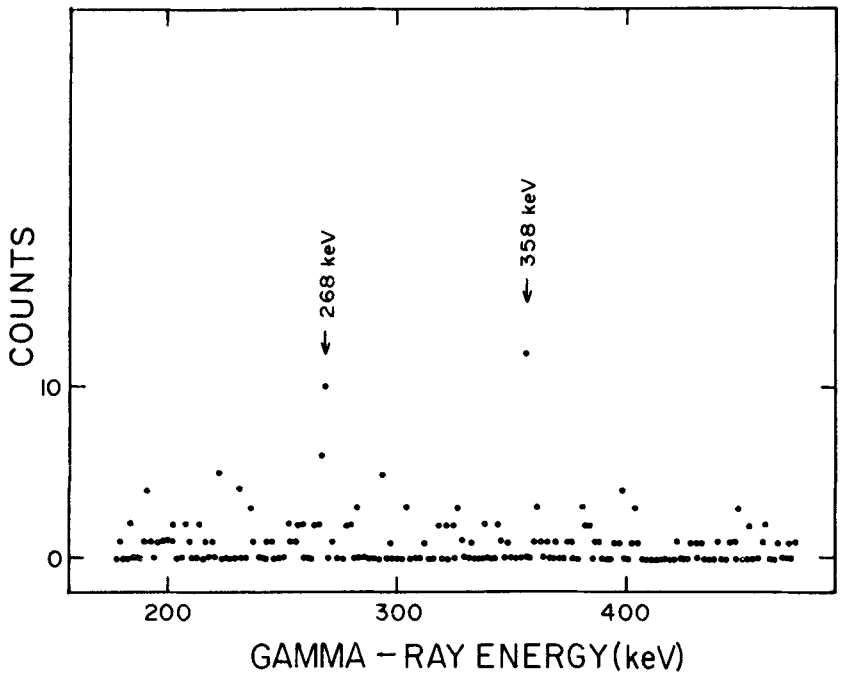

Figure 6. Gamma-ray spectrum (prompt with respect to the beam) in delayed coincidence with any two or more of the six Na(Tl) detectors and any of the transitions in the $K^{\pi} = 9^-$ band which are selected in another HPGe detector. This spectrum clearly shows the 268 keV and 358 keV transitions feeding the isomeric level at 2256 keV.

transition for assumed spins of 15 and 16 for the 2256 keV level. In this calculation the tables of Yamazaki (1967) and the de-orientation parameters from Slaughter *et al* (1984) were used. A comparison of the angular distribution coefficients so calculated with those obtained by Slaughter *et al* (1984) rules out $I^{\pi} = 15^-$ and establishes an assignment of $I^{\pi} = 16^-$ for this level. The $E2$ nature of the 647 keV transition to the 1609 keV (14^-) level of the $K^{\pi} = 9^-$ band and the absence of a transition to the 1328 keV (13^-) level of the same band confirm this assignment.

The ($M1 + E2$) and $E2$ natures of the 268 and 358 keV transitions (see table 1 and figure 6) suggest 17^- and 18^- assignments for the 2524 and 2614 keV levels respectively, if the spins are assumed to increase with increasing excitation energy.

3.3 *g-factor measurement*

The results of the g-factor measurement of the isomeric level at 2256 keV are shown in figure 9 where the function $R(t)$ (see § 2.5) for the 647 keV transition is plotted against time. A similar curve was obtained for the 345 keV transition. The data were least square fitted to obtain a value for the gyromagnetic ratio: $g = 0{\cdot}32 \pm 0{\cdot}05$. Diamagnetic and Knight shift corrections were not applied in view of the rather large statistical uncertainty on the g-factor. A subsequent measurement of this g-factor performed by

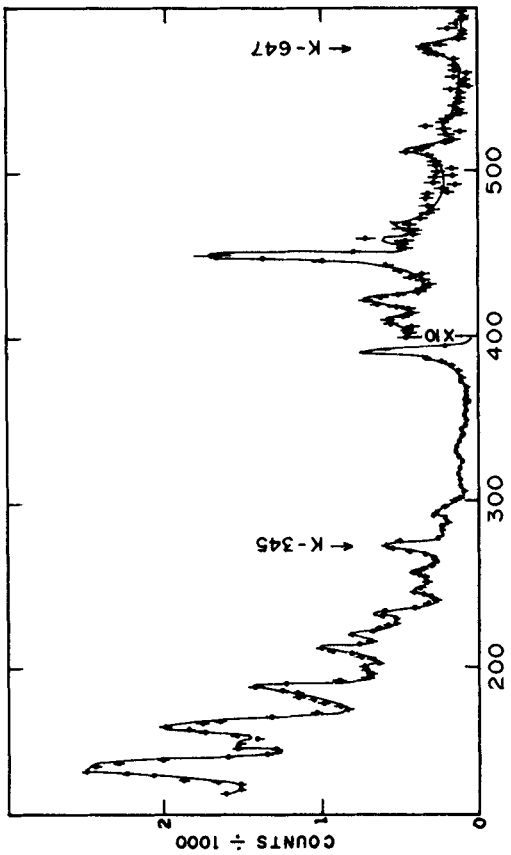

Figure 8. Delayed internal conversion electron spectrum (delayed 15–100 ns with respect to the cyclotron beam burst) coincident with the entire gamma-ray spectrum detected with a Ge(Li) detector. This spectrum essentially shows the conversion lines corresponding to the transitions deexciting the isomeric level (marked in the figure), the transitions in the $K^{\pi}=9^{-}$ band and the 461 keV transition which is also a delayed transition.

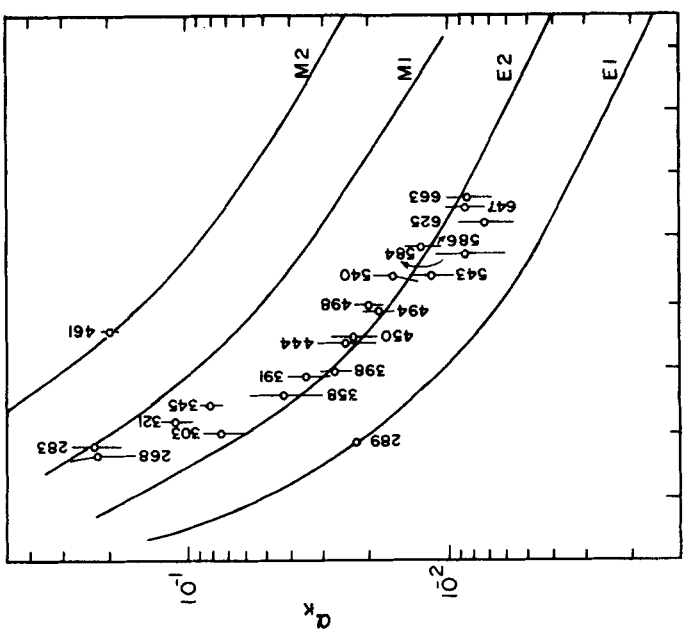

Figure 7. Comparison of the measured K-conversion coefficient α_K with the theoretical values of Hager and Seltzer (1968) for various multipolarities of the transitions, for $Z=75$. The energies of the various transitions for which α_K's have been measured are marked.

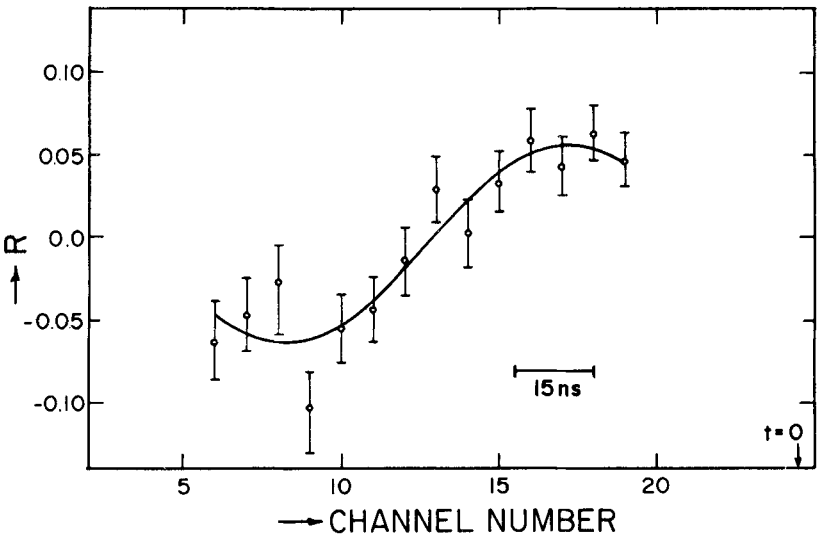

Figure 9. Spin rotation pattern for the 647 keV transition in an external magnetic field of $(1{\cdot}62 \pm 0{\cdot}03)T$. The fractional difference R in the counting rates of the detectors at $\pm 135°$ from the beam direction (see text) is plotted against the channel number denoting the time. The prompt position ($t = 0$) and the scale for time are marked. The solid curve is a fit to the data with $g = +0{\cdot}32$.

Jain *et al* (1985) at the Stockholm cyclotron yielded the result $g = 0{\cdot}239 \pm 0{\cdot}008$, which is $\sim 1{\cdot}5$ standard deviations off from the result reported here. Since the spin-parity of the 2256 keV level is established as 16^-, the magnetic moment of this state is $(5{\cdot}1 \pm 0{\cdot}8)$ nm. The small value of the measured g-factor rules out a $3p\text{-}1n$ character for this level (see § 4).

4. Discussion

The multipolarities assigned to the various transitions on the basis of the present α_K measurements confirm the assignments made by Slaughter *et al* (1984) for the levels in the $K^\pi = 7^+$ and 9^- bands. The level at 2256 keV has been assigned a spin parity of 16^- from the present work in disagreement with the 15^+ assignment made by Slaughter *et al* (1984).

The experimentally known Nilsson single proton and neutron states of high Ω in this mass region are listed in figure 10. The energies are taken from the observed levels in $^{181,183}W$ for the odd neutron states and $^{181,183}Re$ for the odd proton states (Lederer and Shirley 1978; Artna-Cohen 1975). For the $\pi\, 7/2^-[523\uparrow]$ state, which has not been assigned in the Re nuclei, the energy with respect to the $\pi\, 5/2^+[402\uparrow]$ state is taken from the Nilsson diagram [Bohr and Mottelson 1975a (hereafter referred to as BM]. The $K^\pi = 7^+$ and 2^+ bands (see figure 1) are presumably obtained from the parallel and antiparallel coupling of $\nu 9/2^+[624\uparrow]$ and $\pi\, 5/2^+[402\uparrow]$ orbitals. The $K^\pi = 4^-$ band has probably the configuration:] $\pi\, 1/2^-[541\downarrow] \otimes \nu 9/2^+[624\uparrow]$, while the $K^\pi = 9^-$ band is made up of $\pi 9/2^-[514\uparrow] \otimes \nu 9/2^+[624\uparrow]$ (Slaughter *et al* 1984). The 2256 keV level is certainly not a member of any of these bands because of its

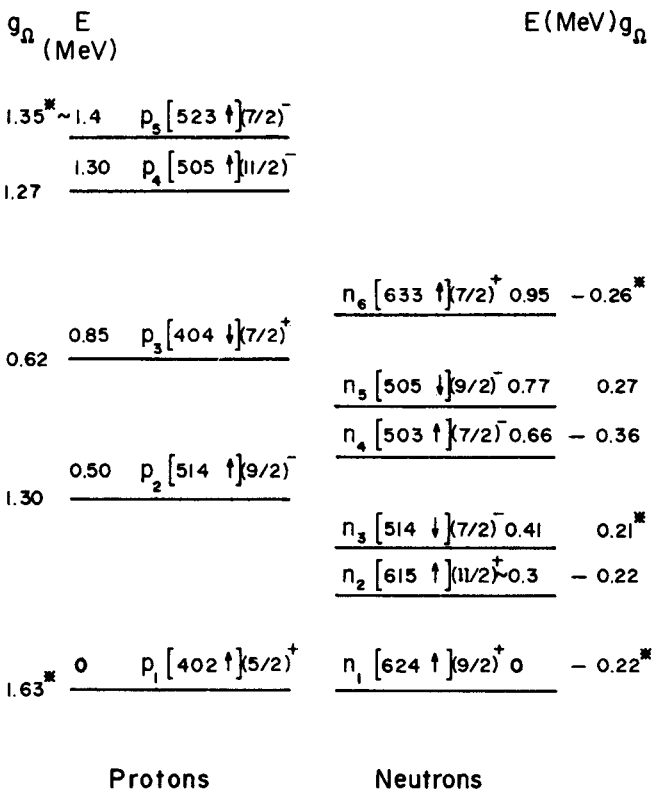

Figure 10. Positions of the proton and neutron states in the mass region $A \approx 182$. The energies are taken from the observed band-head positions in ^{181,183}W, ^{181,183}Re. The position of the $\pi 7/2^-[523\uparrow]$ state is taken from the Nilsson diagram (BM 1975a). The proton and neutron states are marked with p and n respectively with subscripts. These designations are used in table 2. The g_Ω values used in calculating the g-factor for 4-quasi-particle states are also indicated. The numbers with an asterisk are taken from (BM 1975c). The others are calculated (see text).

isomeric nature. For the same reason, it also is a band head. The most probable assignment for this state made by Slaughter *et al* (1984) is: $\{\pi 9/2^-[514\uparrow] \otimes \pi 7/2^-[523\uparrow] \times \pi 5/2^+[402\uparrow] \otimes \nu 9/2^+[624\uparrow]\} K^\pi = 15^+$. It is quite clear that a four quasiparticle configuration is the only one that attains such a large K-value. However, the question whether it is a $3p$-$1n$ or $1p$-$3n$ configuration cannot be determined from the previous studies. The g-factors expected for several high K-band heads that can be constructed from the orbitals listed in figure 10, can be calculated and compared with the experimental value. The g-factor of the band head ie a state with $I = K$, is given by (BM 1975b)

$$g_{I=K} = \frac{1}{(I+1)}[g_K K + g_R], \tag{4}$$

where g_K is the intrinsic g-factor and g_R the rotational g-factor. g_R values in this region vary between 0·2 and 0·4 (BM 1975c) and a value 0·35 has been used in the present calculation. As can be seen from (4), g_I is not very sensitive to g_R. The intrinsic g-factor

for the four-particle configuration, where all the individual Ω's are coupled in parallel is given by

$$g_K K = \sum_i g_{\Omega i}\Omega_i, \tag{5}$$

where $g_{\Omega i}$ are the intrinsic g-factors of the various single particle configurations, making the four-particle configuration. g_Ω for some of the proton and neutron states listed in figure 10 are tabulated by BM (1975c). These values, shown by an asterisk in figure 10, have been used in the calculation. For the other single particle configurations, the g_Ω were calculated using the Nilsson wavefunctions (Nilsson 1955) for the appropriate deformation viz. $\delta = 0{\cdot}25$ (BM 1975d) and a quenched value for the spin g-factor $g_s = 0{\cdot}7 g_{s,\text{free}}$ for both protons and neutrons. The g-factors so calculated for the band-heads of the four-quasiparticle configurations considered by Slaughter *et al* (1984) and for all the possible $K^\pi = 16^-$ configurations that can be formed from the proton and neutron orbitals listed in figure 10, are presented in table 2. The estimated uncertainty in the calculated g-factors is $\pm 0{\cdot}05$. As can be seen from table 2, the $3p$-$1n$ configurations have rather large g-factors ranging from 0·7 to 1·1, while the experimental value is $0{\cdot}32 \pm 0{\cdot}05$ in the present experiment and $0{\cdot}239 \pm 0{\cdot}008$ in the work of Jain *et al* (1985). Thus a $3p$-$1n$ character for the 2256 keV level can definitely be ruled out. Of the various $1p$-$3n$ configurations, the first four listed in table 2 are consistent with the measured g-factor. However, the configurations in 2nd, 3rd and 4th line in table 2 are expected to lie at higher energies as compared to the configuration 1. Thus we arrive at the most probable configuration for this four-quasiparticle state as:

$$\{\pi 9/2^-[514\uparrow] \otimes \nu 9/2^+[624\uparrow] \otimes \nu 7/2^-[514\uparrow] \otimes \nu 7/2^-[503\uparrow]\}_{K^\pi = 16^-}.$$

However, there is a major discrepancy. The 345keV ($M1 + E2$) and 647 keV $E2$

Table 2. Calculated values of the gyromagnetic ratio, g, for various 4-quasiparticle band-heads formed from the several proton and neutron states shown in figure 10. The $3p$-$1n$ and $1p$-$3n$ configurations are shown on the left and the right respectively. The subscripts on p and n refer to the single particle numbers shown in figure 10.

$3p$-$1n$ configurations			$1p$-$3n$ configurations		
Configuration	$K = I$	Calculated value of g	Configuration	$K = I$	Calculated value of g
$p_1p_2p_3n_1$	15^-	0·72	$p_2n_1n_3n_4$	16^-	0·28
$p_1p_2p_5n_1$	15^+	0·88	$p_2n_4n_5n_6$	16^-	0·31
$p_1p_3p_4n_1$	16^-	0·74	$p_4n_3n_4n_6$	16^-	0·35
$p_1p_2p_4n_3$	16^-	1·11	$p_5n_1n_3n_5$	16^-	0·36
$p_3p_4p_5n_3$	16^-	0·90	$p_2n_3n_5n_6$	16^-	0·43
$p_1p_2p_3n_2$	16^-	0·66	$p_3n_1n_5n_6$	16^-	0·10
$p_1p_2p_4n_4$	16^-	0·94	$p_3n_2n_3n_6$	16^-	0·07
$p_3p_4p_5n_4$	16^-	0·76	$p_3n_2n_4n_6$	16^-	−0·05
$p_2p_3p_5n_5$	16^-	0·84	$p_1n_1n_2n_3$	16^-	0·17
$p_1p_4p_5n_5$	16^-	1·02	$p_1n_2n_5n_6$	16^-	0·21
			$p_1n_1n_2n_4$	16^-	0·06
			$p_5n_1n_4n_5$	16^-	0·24
			$p_5n_2n_3n_4$	16^-	0·19

transitions are highly K-forbidden, with the initial and final K-values for the levels involved in these transitions being $K^\pi = 16^-$ and 9^-, respectively. The $M1$ part of the 345 keV transition is 6 times K-forbidden while its $E2$ component and 647 keV transition are 5 times K-forbidden. The retardation factors, relative to Weisskopf estimate, for the $M1$ and $E2$ components of the 345 keV transition, calculated from the half-life of $T_{1/2} = (88 \pm 8)$nsec (Slaughter *et al* 1984) and the $M1/E2$ mixing ratio obtained from α_K measured in the present work, are $\sim 10^6$ and 154 ± 30 respectively. Similarly the 647 keV $E2$ radiation is retarded by a factor 2600 ± 400. The systematics of K-forbidden transitions in well-deformed nuclei show that each fold of K-forbiddenness brings in a retardation factor of $\approx 10^{1.5}$ to $\approx 10^2$ (BM 1975e). Thus the $E2$ transitions are expected to be retarded by factors of up to $10^{7.5}$ to 10^{10}, while the experimental retardation factors are only $\sim 10^2$ to 10^3. Such a large discrepancy in the retardation factors for these highly K-forbidden transitions cannot be easily reconciled with an axially symmetric structure for the nucleus, where K is a good quantum number. A similar discrepancy has also been noted in the highly K-forbidden transitions in ^{182}Os (Pedersen *et al* 1985). One possible explanation of such a discrepancy is the deviation of the nucleus from axial symmetry. In such a triaxial case, K is no longer a good quantum number and states can be expanded as a linear combination of several K-states. A K-admixture in either or both of the initial and final states involving the transition, such that a component exists with $\Delta K = 2$, can explain the rather small value of the retardation of the transitions. A 3% admixture in the amplitude of $K^\pi = 11^-$ state in the 2256 keV state, for example, can explain the observed life time. The 'oblateness' brought in by the four unpaired particles can bring in a triaxiality for the nucleus in this configuration. Nuclei in the mass region $A \sim 182$ are rather soft to γ-deformation as evidenced by the low excitation energy of the γ-band head at 890 keV in ^{182}Os (Lederer and Shirley 1978). Further, the high spin members of a rotational band (the $K^\pi = 9^-$ band in this case) of a nucleus with even a small axial asymmetry can have components with $K \approx I$ (BM 1975f). A calculation of the triaxiality brought about by such effects is of interest in explaining not only the present result but also the observation of Pedersen *et al* (1985) for ^{182}Os.

5. Conclusions

The properties of the isomeric level at 2256 keV in ^{182}Re have been determined in the present work. An unambiguous spin parity assignment of 16^- has been made for this level. Further, the g-factor of this level was measured to be $g = 0{\cdot}32 \pm 0{\cdot}05$. On the basis of the g-factor, this level can be identified as the band head of a $K^\pi = 16^-$ band with the configuration:

$$\{\pi 9/2^-[514\uparrow] \otimes \nu 9/2^+[624\uparrow] \otimes \nu 7/2^-[514\uparrow] \otimes \nu 7/2^-[503\uparrow]\}_{K=16^-}.$$

However, the gamma transitions deexciting this level do not show the expected retardation, being $\sim 10^5$ to 10^7 times faster than expected for these highly K-forbidden transitions. It was suggested that this may be explained if the nucleus has a triaxial shape in the initial and/or the final states involving these transitions. It is very important that theoretical estimates of such triaxiality be made. A study of the excited states with higher spins in the $K^\pi = 9^-$ and 16^- bands, through heavy-ion induced

reactions, where higher angular momentum states can be populated, will be of interest.

Acknowledgements

The authors wish to thank S K Ambardekar for the fabrication of the Solenoid electron spectrometer, S C Vaidya for help with the Si(Li) detectors, P J Bhalerao, M R Datta Mazumdar, D A Gothe and M Y Vaze for help during all stages of the experiment. D Indumathi and C R Bhuinya participated in parts of the experiment. Thanks are due to S N Chintalapudi and the staff of VECC for their help at the cyclotron centre at Calcutta.

References

Agarwal Y K, Bhuinya C R, Baba C V K, Bhattacherjee B K, Bhattacharya D, Bhowmik R K, Datar V M and Jain H C 1985 *Proc. of DAE Symp. Nucl. Phys.*, Jaipur, India **B28** C20

Artna-Cohen A 1975 *Nuclear Data Sheets* **16** 267

Bohr A and Mottelson B R 1975a *Nuclear Structure* Vol. II (Reading, Mass: Benjamin) p. 224

Bohr A and Mottelson B R 1975b *Nuclear Structure* Vol. II (Reading, Mass: Benjamin) p. 56

Bohr A and Mottelson B R 1975c *Nuclear Structure* Vol. II (Reading, Mass: Benjamin) p. 303

Bohr A and Mottelson B R 1975d *Nuclear Structure* Vol. II (Reading, Mass: Benjamin) p.133

Bohr A and Mottelson B R 1975e *Nuclear Structure* Vol. II (Reading, Mass: Benjamin) p. 144

Bohr A and Mottelson B R 1975f *Nuclear Structure* Vol. II (Reading, Mass: Benjamin) p. 192

Burson S B, Daly P J, Goudsmit P F A and Klasse A A C 1973 *Nucl. Phys.* **A204** 337

Frauenfelder H and Steffen R M 1965 in α, β, γ *spectroscopy* Vol. II p. 997 (ed.) K Siegbahn (Amsterdam: North Holland Publishing Company)

Hager H S and Seltzer E C 1968 *Nucl. Data* **A4** 397

Hjorth S A , Ryde H and Skaanberg B 1968 *Ark. Fys.* **38** 537

Jain H C, Norlin L, Rosengard U, Filevich A and Dafni E AFI (Stockholm University) Biennial report 1984–85, p. 132

Lederer C M and Shirley V S 1978 *Tables of Isotopes* Seventh Edition (New York: John Wiley and Sons Inc.)

Medsker L R, Emery G T, Singh P P, Beach L A and Gossett C R 1971 *Bull. Am. Phys. Soc.* **16** 515

Nilsson S G 1955 *K. Dan. Vid. Sel. Mat. Fys. Medd.* **29** No 16

Pedersen J, Back B B, Bjørnholm S, Borggren J, Diebel M, Sletten G, Azgui F, Emling H, Grein H, Seiler-Clark G, Spreng W, Wollersheim H J, Walker P and Aberg S 1985 *Phys. Rev. Lett.* **54** 306

Slaughter M F, Warner R A, Khoo T L, Kelly W H and McHarris Wm C 1984 *Phys. Rev.* **C29** 114

Singh P P, Medsker L R, Emery G T, Beach L A and Gossett C R 1974 *Phys. Rev.* **C10** 656

Svahn B, Bergman C, Johansson A, Nyman B, Dietrich W and Ibrahiem N 1973 *Phys. Scr.* 7 257

Yamazaki T 1967 *Nuclear Data* **A3** 1